Review of Scientific Instruments

Consideration of signal to noise ratio for an imaging bolometer for ITER

Cite as: Rev. Sci. Instrum. **92**, 043534 (2021); https://doi.org/10.1063/5.0043201
Submitted: 07 January 2021 • Accepted: 22 March 2021 • Published Online: 12 April 2021

Byron J. Peterson, Roger Reichle, Santosh Pandya, et al.

Review of Scientific Instruments ARTICLE scitation.org/journal/rsi

Consideration of signal to noise ratio for an imaging bolometer for ITER

Cite as: Rev. Sci. Instrum. 92, 043534 (2021); doi: 10.1063/5.0043201
Submitted: 7 January 2021 • Accepted: 22 March 2021 •
Published Online: 12 April 2021

Byron J. Peterson,[1,2,a)] Roger Reichle,[3] Santosh Pandya,[3] Martin G. O'Mullane,[4] and Kiyofumi Mukai[1,2]

AFFILIATIONS

[1] National Institute for Fusion Science, 322-6 Oroshi-cho, Toki 509-5292, Japan
[2] SOKENDAI (Graduate School for Advanced Studies), 322-6 Oroshi-cho, Toki 509-5292, Japan
[3] ITER Org., Route de Vinon-sur-Verdon, CS 90 046, 13067 St. Paul Lez Durance Cedex, France
[4] Department of Physics SUPA, University of Strathclyde, Glasgow G4 0NG, United Kingdom

Note: Paper published as part of the Special Topic on Proceedings of the 23rd Topical Conference on High-Temperature Plasma Diagnostics.
[a)] **Author to whom correspondence should be addressed:** peterson.byron@nifs.ac.jp

ABSTRACT

An infrared imaging video bolometer (IRVB) is proposed for ITER having a tangential view of the entire ITER cross section. For the initial estimate of the signal level, a 840 m^3 plasma is assumed to uniformly radiate 67.3 MW. A more detailed estimate of the signal strength is provided by synthetic images based on radiation data from SOLPS and SANCO models for the edge and core plasma, respectively. The Pt foil used as the radiation absorber would have the dimensions of 7 × 9 cm^2 and a thickness of 16 μm that will stop 95% of the radiated power. Two different InSb based IR cameras having a sensitivity of 15 mK are considered for measuring the temperature rise of the foil due to the radiation. The first has 1280 × 1024 $pixel^2$ and a frame rate of 105 fps. The second has 640 × 512 $pixel^2$ and a frame rate of 1000 fps. The resulting IRVBs have 40 × 30 $pixel^2$, 10 ms time resolution, and a signal to noise ratio (SNR) of 17 and 20 × 15 $pixel^2$, 3 ms time resolution, and a SNR of 35, respectively. The synthetic image data give SNRs of 30 and 59, respectively.

I. INTRODUCTION

The InfraRed imaging Video Bolometer (IRVB)[1,2] represents an alternative to resistive bolometers[3,4] for diagnosing the radiated power distribution in a fusion reactor such as ITER.[5] The IRVB consists of an aperture collimated foil that absorbs broadband radiation from the plasma. The resulting temperature rise of the foil is measured by an IR camera placed outside the vacuum vessel. Experiments on JT-60U[6] and modeling of JT-60SA[7] have demonstrated the ability of an IRVB with a tangential view to produce two-dimensional poloidal profiles of the radiated power based on the assumption of axis-symmetry. Previous work addressing an IRVB for ITER focused on the lines of sight (LOS) distribution for various IRVB locations.[8] In this paper, we consider the signal to noise ratio (SNR) for the IRVB placement from that study[8] having the best LOS distribution. However, the placement of the IRVB in this paper is an idealized location that does not take into account any environmental constraints or ITER, in particular, no restrictions from the space envelope available for implementing it.

II. IRVB DESIGN

A. IR camera parameters

The IR camera parameters used in the design are based on commercially available InSb detector-based IR cameras. Three IR camera and IRVB configurations are considered and designated "A1" (high spatial resolution), "A2" (medium spatial resolution), and "B" (high temporal resolution). The IR camera parameters N_{pix}, number of IR camera pixels, σ_{IR}, the noise equivalent temperature of the IR camera, and f_{IR}, frame rate of the IR camera, are given in Table I. The σ_{IR} value used is twice the manufacturer's value to take into account signal losses through the periscope between the IR camera and the foil.

B. Bolometer camera design

The IRVB aperture is located in (x, y, z) coordinates (x—major radial, y—toroidal, z—vertical) at (8.5, 0, 0) m. The foil dimensions are 9 cm (height), 7 cm (width), and 0.0016 cm (thickness, t_f). The determination of the required foil thickness is discussed in Sec. IV.

TABLE I. IRVB parameters.

IRVB		A1	A2	B
		IR camera parameters		
N_{pix}		1024 × 1280		512 × 640
f_{IR}	1/s	105		1000
σ_{IR}	K	1.5 × 10−2		
		Pt foil parameters		
K	W/K m		71.6	
K	m^2/s		25.6 × 10−6	
t_f	m		16 × 10−6	
		IRVB parameters		
N_{IR}		949 682		232 287
A_f	m^2	0.06 × 0.08		
N_{bol}		30 × 40	24 × 32	15 × 20
f_{bol}	1/s	100		333
A_{bol}	m^2	4×10^{-6}	6.25 × 10−6	16×10^{-6}
A_{ap}	m^2	9×10^{-6}	14.1 × 10−6	36×10^{-6}
l_{ap-f}	m		0.078	
θ	deg		20	
l_{plasma}	m		10	
S_{IRVB}	W/m^2	3.4	2.7	6.7
		Plasma parameters		
P_{rad}	W		6.727×10^7	
V_{plasma}	m^3		840	
		Signal levels and signal to noise ratios		
S_{signal}	W/m^2	58.8	91.9	235
S/N		17	34	35
S_{core}	W/m^2	102.0		390.8
S_{edge}	W/m^2	53.4		116.5
S_{total}	W/m^2	103.2		395.0
S/N		30.4		59.0

The foil center is at (8.5599, −0.0505, 0) m, and the centers of the foil sides are at (8.5382, −0.0780, 0) and (8.5815, −0.0230, 0) m. The distance from the foil to the aperture, l_{ap-f}, is 0.078 m. The major radius of tangency of the line passing through the centers of the foil and of the aperture is 5.9192 m. Typically, the 5 mm edge of the foil is not used in the analysis due to high temperature gradients at the foil edge leaving 6 × 8 cm^2 for the measurement. The aperture area, A_{ap}, is taken to be 2.25 × A_{bol}, the bolometer pixel area, which varies with the design as shown in Table I, in order to increase the signal level. Previous work has shown that oversizing A_{ap} relative to A_{bol} by a factor of 2.25 will only slightly degrade the tomographic inversion.[7] The field of view (FoV) of the IRVB is shown in the CAD image in Fig. 1.

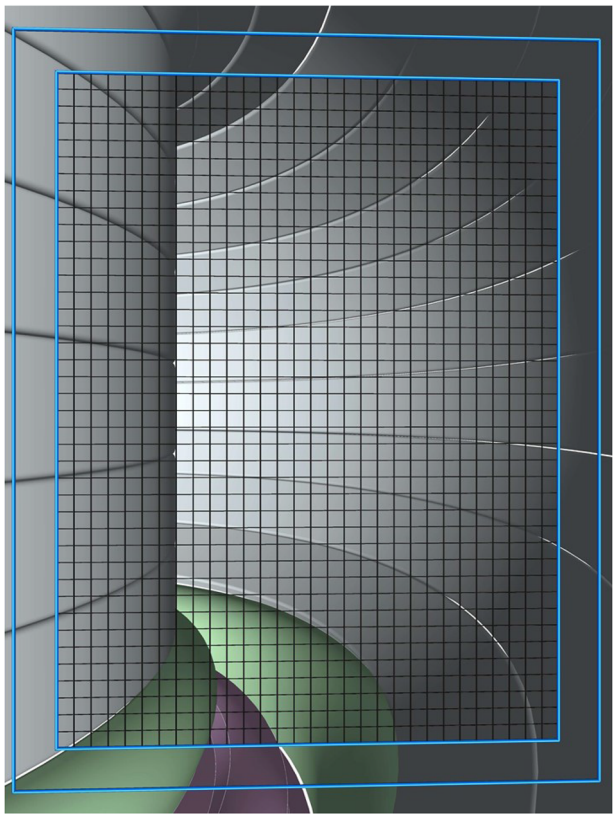

FIG. 1. CAD image of IRVB FoV. Outer blue line shows the edge of foil, and inner blue line shows the edge of the foil region used for measurement. Gray grid shows individual bolometer pixels for case A1.

III. SIGNAL TO NOISE ESTIMATION

A. Noise equivalent power estimation

The noise equivalent power density (NEPD), S_{IRVB}, of the IRVB is given by the following equation:

$$S_{IRVB} = \frac{\eta_{IRVB} N_{bol}}{A_f} = \frac{\sqrt{10} k t_f \sigma_{IR}}{\sqrt{f_{IR} N_{IR}}} \sqrt{\frac{N_{bol}^3 f_{bol}}{A_f^2} + \frac{N_{bol} f_{bol}^3}{5\kappa^2}}, \quad (1)$$

with N_{bol} being the number of bolometer channels, A_f being the utilized area of the foil, f_{bol} being the effective frame rate of the bolometer, N_{IR} being the utilized number of IR camera pixels, k being the thermal conductivity of the foil, and κ being the thermal diffusivity of the foil, all of which are given in Table I.[2] f_{bol} is chosen to match the measurement requirements of 10 and 3 ms for the Iter bolometer.[5] N_{IR} is smaller than N_{pix} because the IR camera views the whole foil and part of the frame in order to locate the foil in the IR camera FoV, while the IR camera pixels used in the analysis, N_{IR}, are limited to those viewing the 6 × 8 cm^2 center of the foil plus one additional row of bolometer pixels around this border. This additional row of bolometer pixels around the edge is needed to calculate the second spatial derivative of the foil temperature for the Laplacian term of the foil power balance equation used to solve for the incident power from the foil temperature distribution.

B. Signal estimation

1. Rough signal estimation

The radiated power density at the foil, S_{signal}, can be given approximately by the following equation:

$$S_{signal} = \frac{P_{signal}}{A_{bol}} = \frac{A_{bol} A_{ap} \cos^4 \vartheta P_{rad} l_{plasma}}{A_{bol} 4\pi l_{ap-f}^2 V_{plasma}}, \quad (2)$$

with $A_{bol} = A_f/N_{bol}$ being the area of the bolometer pixel, θ being the average incident angle of the sightline with respect to the foil, P_{rad} being the total radiated power, l_{plasma} being the average length of the sightline through the plasma, and V_{plasma} being the volume of the plasma, all of which are given in Table I. P_{rad} is taken from the total radiated power predicted by the SOLPS and SANCO codes as described in Sec. III B 2. A_{ap} is taken to be $2.25 \times A_{bol}$ in order to increase the signal level. Previous work has shown that oversizing A_{ap} relative to A_{bol} by a factor of 2.25 will only slightly degrade the tomographic inversion.[7] Combining Eqs. (1) and (2), the signal to noise ratio (SNR) can be given as shown in Table I.

2. Signal estimation from synthetic images

A more precise estimation of the expected signal strength (in W), P_i, for detector i, can be obtained from synthetic images derived from estimates of the spatial distribution of the radiated power density (in W/m^3), U_j, from plasma cell j, from SANCO (core) and SOLPS (edge) simulation codes[9] for the ITER standard 15 MA reference plasma scenario[10] by using the projection matrix, T_{ij}, calculated from the IRVB geometry,[7]

$$P_i = \sum_j \frac{V_{ij}\Omega_{ij}}{4\pi} U_j = \sum_j T_{ij} U_j, \quad (3)$$

with V_{ij} being the intersecting volume between the FoV of the ith detector and the jth plasma cell and Ω_{ij} being the solid angle of the ith detector with respect to the jth plasma cell. The plasma poloidal cross section shown is divided into 219 (horizontal) × 465 (vertical) = 101 835 cells having dimensions of 2 × 2 cm^2 in the region, which ranges 4.02 m ≤ R ≤ 8.4 m and −4.58 m ≤ Z ≤ 4.72 m and which includes all of the plasma region inside the first wall. Core radiation data from SANCO are defined for the 30 regions between the flux surfaces. The radiation from these cells is resampled onto the 2 cm plasma grid. Edge and divertor radiation from SOLPS is defined for 8866 trapezoidal cells having a minimal dimension of 2 mm. Therefore, these data were first resampled onto a 1 mm square grid and then resampled onto the 2 cm grid. The reference profiles utilized emit 65 MW of total radiated power for a total fusion power of 400 MW. The impurity mix considered by both SOLPS and SANCO was 2% Be, 10^{-5} W, 0.1% Ne, and 0.1% Ar.[9]

The projection matrix, T_{ij}, having dimension of 1200 × 101 835 for case A1 (high spatial resolution) and 300 × 101 835 for case B (high temporal resolution) was then calculated by integrating along each IRVB detector's line of sight in steps of 2 cm while dividing the FoV into subFoVs having a maximum dimension of 2 cm. Integration was halted for each subFoV when the first wall was intersected. Then, using the resampled radiation distributions, U_j, and the projection matrix, $T_{i,j}$, the synthetic images of the radiated power

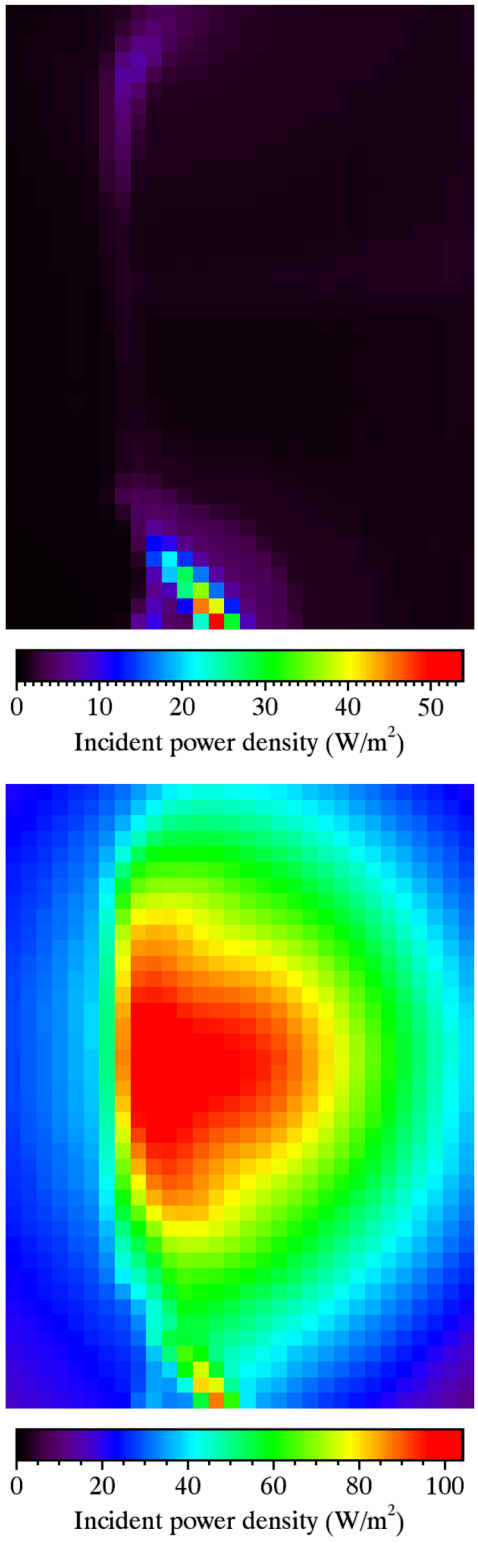

FIG. 2. Synthetic images for the IRVB in case A1 (high spatial resolution) for edge radiation (upper) and total (core + edge) radiation (lower).

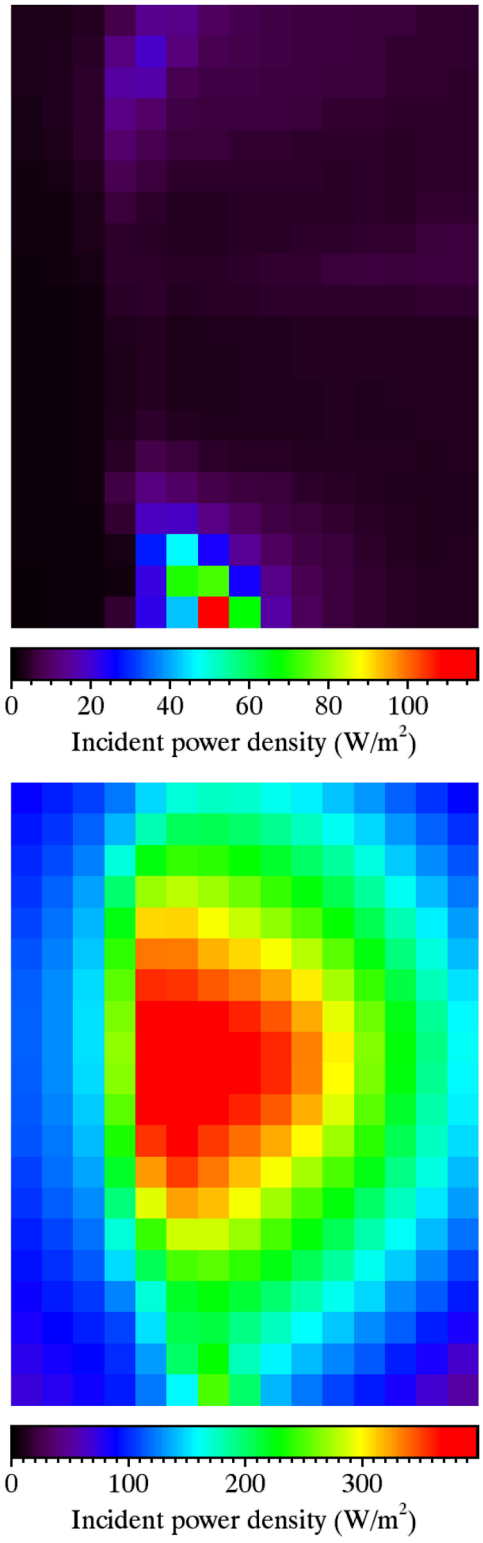

FIG. 3. Synthetic images for the IRVB in case B (high temporal resolution) for edge radiation (upper) and total (core + edge) radiation (lower).

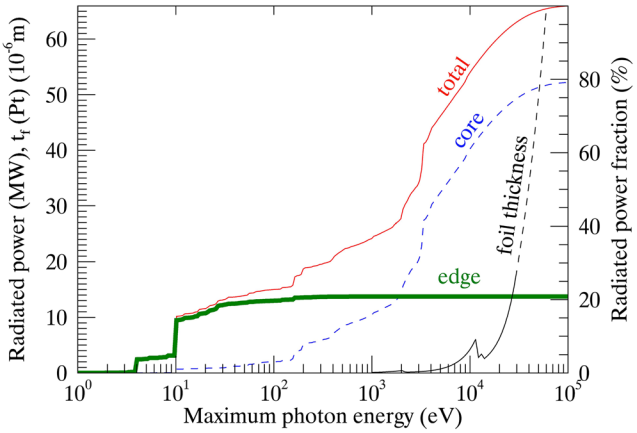

FIG. 4. Radiated power and radiated power fraction for edge (green thick line), core (blue dashed line), and total (core + edge) (red line) vs maximum photon energy, and Pt foil thickness (attenuation length)[11] (black dashed line is extrapolation beyond 18 μm, 30 keV) vs photon energy.

density, $S_i = P_i/A_{bol}$, incident on the two-dimensional bolometer detector array were calculated using Eq. (3). The synthetic images are shown for the edge and total (core + edge) radiation in Fig. 2 for case A1 (high spatial resolution) and in Fig. 3 for case B (high temporal resolution).

IV. REQUIRED FOIL THICKNESS

The radiated power data from the SANCO and SOLPS codes are provided not only in terms of spatial location but also in terms of photon energy. In Fig. 4, the radiated power fraction vs maximum photon energy is plotted for both core and edge radiation by integrating over the radiating volumes. When combined with data on the attenuation length of photons vs photon energy for Pt,[11] which is also shown in Fig. 4, this permits an evaluation of the minimum foil thickness needed to absorb a certain fraction of the radiated power,

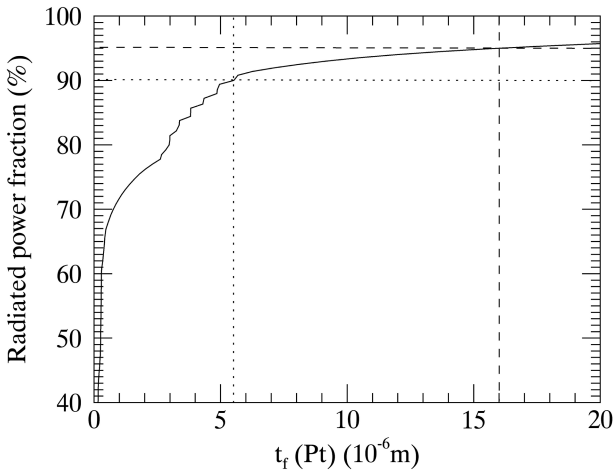

FIG. 5. Total radiated power fraction vs Pt foil thickness.

as shown in Fig. 5. From this plot, it can be seen that a 16 μm Pt foil is necessary to stop 95% of the total radiated power. Therefore, this is the foil thickness used in this study.

V. CONCLUSIONS AND DISCUSSION

The rough estimate of the signal level, while relying on somewhat arbitrary values of θ and l_{plasma}, gives numbers consistent with the more accurate synthetic image calculation. The SNR for case A1 (high spatial resolution) is a little low, and therefore, case A2 (medium spatial resolution) with a lower number of bolometer pixels was considered with a rough estimate of the signal. From Fig. 4, it can be seen that 95% of the radiation from the edge has energies below 100 eV and 95% of the radiation from the core has energies above 100 eV. From Fig. 5, it can be seen that a 5.6 μm foil would measure 90% of the radiated power. Reducing the foil thickness by a factor of 3 would improve the sensitivity and SNR by a factor of 3 according to Eq. (1).

Taking these three points into account, one can imagine that the optimal measurement of the radiation from ITER would use two IRVBs, one having the parameters of case B (high temporal resolution) to measure the core radiation with 3 ms time resolution but with a lower spatial resolution to match the 20 cm measurement requirement of the core.[5] The other could match the IR camera parameters and f_{bol} of case A1 (high spatial resolution) with a 4–5 μm foil for higher sensitivity and view the divertor directly from a lower part of an equatorial port to avoid viewing through the center of the core plasma from which the high energy x rays are emanating. The increase in sensitivity could be used to increase N_{bol} in order to meet the higher spatial resolution requirements of the divertor while still maintaining a sufficient SNR. However, in order to determine if such an arrangement could satisfy the spatial measurement requirements, tomographic modeling, which is planned for the future, must be carried out. In addition, other scenarios and more realistic IRVB placement should be considered. In addition, the evaluation of the necessary foil thickness was made considering the total power radiated by the plasma and did not consider the FoV of the IRVB. In the future, this analysis should be applied to the total power absorbed by the foil in order to determine the appropriate foil thickness for each IRVB's foil. Additional future work should include modeling of the effect of neutron and gamma heating of the foil.

ACKNOWLEDGMENTS

B.J.P. would like to thank R. Sano of the National Institutes for Quantum and Radiological Science and Technology (Japan) for advice regarding the modification of the projection matrix code and H. Kojima of the National Institute for Fusion Science (Japan) (NIFS) for creating Fig. 1. This work was completed with support from NIFS budget Grant No. NIFS16ULHH026. The contributions of the first author to this article were carried out as an ITER Scientist Fellow and were partially supported by the ITER Organization.

The views and opinions expressed herein do not necessarily reflect those of the "ITER Organization."

DATA AVAILABILITY

The data that support the findings of this study are available from the corresponding author upon reasonable request.

REFERENCES

[1] B. J. Peterson, "Infrared imaging video bolometer," Rev. Sci. Instrum. **71**(10), 3696–3701 (2000).
[2] B. J. Peterson *et al.*, "Calibration and sensitivity of the infrared imaging video bolometer," Rev. Sci. Instrum. **74**(3), 2040–2043 (2003).
[3] H. Meister *et al.*, "Current status of the design of the ITER bolometer diagnostic," Fusion Eng. Des. **120**, 21–26 (2017).
[4] H. Meister *et al.*, "An alternative geometry for bolometer sensors for use at high operating temperatures," Fusion Eng. Des. **112**, 579–586 (2016).
[5] A. J. H. Donne *et al.*, "Chapter 7: Diagnostics," Nucl. Fusion **47**(6), S337–S384 (2007).
[6] Y. Liu *et al.*, "Application of tomographic imaging to multi-pixel bolometric measurements," Plasma Fusion Res. **2**, S1124 (2007).
[7] R. Sano *et al.*, "Conceptual design of imaging bolometer for use of computed tomography in JT-60SA," Rev. Sci. Instrum. **88**, 053506 (2017).
[8] B. J. Peterson *et al.*, "Imaging bolometer for a burning plasma experiment," in *European Conference Abstracts* (European Physical Society, 2003), Vol. 27A, p. 4.067.
[9] M. G. O'Mullane, "Energy resolved radiated power simulations for ITER bolometer study—Compatible core and edge predictions," private communication, 2016, available at https://user.iter.org/?uid=RTPL2V.
[10] A. R. Polevoi *et al.*, "ITER confinement and stability modelling," J. Plasma Fusion Res. Ser. **5**, 82–87 (2002).
[11] B. L. Henke, E. M. Gullikson, and J. C. Davis, "X-ray interactions: Photoabsorption, scattering, transmission, and reflection at E = 50-30,000 eV, Z = 1-92," At. Data Nucl. Data Tables **54**(2), 181–342 (1993), available at http://henke.lbl.gov/optical_constants/.